Research Article

JOURNAL OF HEPATOLOGY

Laminin-332 sustains chemoresistance and quiescence as part of the human hepatic cancer stem cell niche

Olivier Govaere[1,*], Jasper Wouters[1], Michaela Petz[2], Yves-Paul Vandewynckel[3], Kathleen Van den Eynde[1], Anke Van den broeck[4], Stefaan Verhulst[5], Laurent Dollé[5], Lies Gremeaux[6], An Ceulemans[1], Frederik Nevens[7], Leo A. van Grunsven[5], Baki Topal[4], Hugo Vankelecom[6], Gianluigi Giannelli[8], Hans Van Vlierberghe[3], Wolfgang Mikulits[2], Mina Komuta[1], Tania Roskams[1]

[1]*Department of Imaging and Pathology, KU Leuven and University Hospitals Leuven, Leuven, Belgium;* [2]*Department of Medicine I, Institute of Cancer Research, Medical University of Vienna, Vienna, Austria;* [3]*Department of Hepatology & Gastroenterology, Ghent University, Ghent, Belgium;* [4]*Department of Abdominal Surgery, KU Leuven and University Hospitals Leuven, Leuven, Belgium;* [5]*Department of Biomedical Sciences, Liver Cell Biology Laboratory, Vrije Universiteit Brussel, Brussels, Belgium;* [6]*Department of Development and Regeneration, KU Leuven, Leuven, Belgium;* [7]*Department of Hepatology, KU Leuven and University Hospitals Leuven, Leuven, Belgium;* [8]*Department of Medical Biosciences and Human Oncology, Padiglione Semeiotica Medica, Bari, Italy*

Background & Aims: Cancer stem cells (CSCs) are thought to be persistent in tumours due to their chemoresistance and to cause relapse and metastasis. Hepatic carcinomas displaying hepatic progenitor cell (HPC) features have been associated with a poor prognosis, though it remains unclear how CSCs relate to these different histological subtypes.

Methods: Candidate CSCs were isolated using the side population (SP) technique from primary tissue samples diagnosed as keratin (K)19-negative or -positive hepatocellular carcinoma (HCC) or as combined hepatocellular/cholangiocarcinoma and analysed for gene and protein expression. The effect of laminin-332 was analysed *in vitro* by using HCC cell lines and *in vivo* using a xenograft mouse model.

Results: The size of the SP correlated with the degree of HPC features found in human hepatic cancer, and also showed an elevated mRNA expression of biliary/HPC markers and the extracellular matrix marker *LAMC2*, the gene encoding the laminin γ2-chain. Immunopositivity for the γ2-chain of laminin-332 was seen in the extracellular matrix surrounding small HPC-like tumour cells with a low proliferation rate. *In vitro*, laminin-332 increased K19 expression, phosphorylated mTOR and decreased phospho-histone H3 expression, indicating reduced cell mitosis. The effect of laminin-332 was enhanced upon mTORC1 inhibition and diminished when inhibiting mTORC1+C2. Resistance to doxorubicin and sorafenib treatment, and the SP fraction increased in the coated condition. *In vivo*, laminin-332 reduced tumour growth and sustained K19 expression.

Conclusions: In this study we identified a prominent role for laminin-332 as part of the specialised CSC niche in maintaining and supporting cell 'stemness', which leads to chemoresistance and quiescence.

© 2015 European Association for the Study of the Liver. Published by Elsevier B.V. All rights reserved.

Keywords: Hepatic cancer; Cancer stem cell; Microenvironment; Niche; Phenotype switching; Extracellular matrix; ATP-binding cassette transporters.
Received 8 January 2015; received in revised form 21 October 2015; accepted 10 November 2015; available online 17 November 2015

* Corresponding author. Address: Translational Cell and Tissue Research, Department of Imaging and Pathology, KU Leuven and University Hospitals Leuven, Minderbroedersstraat 12, B3000 Leuven, Belgium. Tel.: +32 16 336588; fax: +32 16 336640.
E-mail address: olivier.govaere@med.kuleuven.be (O. Govaere).

Abbreviations: ABC, ATP-binding cassette; CC, cholangiocellular carcinoma; CSC, cancer stem cell; FFPE, formalin-fixed paraffin-embedded; FSC-A, Forward Scatter Area; HCC, hepatocellular carcinoma; HPC, hepatic progenitor cell; ITGA6, integrin alpha 6; K, keratin; Ln, laminin; MP, main population; pHH3, phosphorylated histone H3; pmTOR, phosphorylated Mammalian Target of Rapamycin; qPCR, quantitative real-time PCR; SP, side population.

Introduction

Resistance to chemo- and radio-therapeutic treatment is a common phenomenon, especially in liver cancer. One possible explanation for this phenomenon is the cancer stem cell (CSC) concept. CSCs are cancer cells that possess characteristics associated with normal stem cells, in particular their ability to give rise to all tumour-derived cell types found in a cancer sample. Such cells are proposed to be persistent in tumours due to their resistance to classical chemotherapeutics and to cause relapse and metastasis. However, although the concept of CSCs is intriguing and a large number of experimental studies support the CSC hypothesis, there are still open questions and room for caution [1]. One debate concerns the origin of CSCs. Does the CSC derive initially from a normal stem cell or from a dedifferentiated cell during tumour progression?

The vast majority of primary liver cancers arise from liver epithelial cells and is classically subdivided into hepatocellular carcinomas (HCCs), cholangiocellular carcinomas (CCs) or combined HCC/CC. An unresolved question regarding liver cancers is which epithelial cells–hepatocytes, cholangiocytes, hepatic progenitor cells (HPCs) or all three– have to be considered as

the cells of origin. Mature hepatocytes and cholangiocytes have an enormous self-renewal capacity and longevity and so meet the requisite to be targets for oncogenesis [2]. HPCs are a target for carcinogenesis as well, since most of the hepatic cancers arise in a background of chronic liver disease where there is an extensive activation of the HPCs (seen as ductular reaction) [3]. In the regenerating liver, HPCs reside in a specialised microenvironment (the so-called niche), where interactions with the extracellular matrix help decide their cell fate: a choice between differentiation, proliferation or maintaining 'stemness'. Laminins (Ln) are a large family of extracellular matrix proteins mainly distributed along the basement membrane and are comprised of three different chains (α, β and γ). They have been described to be part of the specialised HPC niche in both human and mouse, where they are thought to play a crucial role in sustaining HPC features [4,5]. In the last decade, many laboratories have underlined the role of the isoform-5, more recently renamed as Ln-332, in promoting tumour progression and dissemination [6]. Our group previously showed that the γ2-chain of Ln-332 in particular was highly elevated in HCCs expressing the biliary/HPC marker keratin (K)19 [7]. Other reports described the γ2-chain as a poor prognostic factor for patients diagnosed with a HCC or an intrahepatic CC [8,9]. Ln-332 can interact with the integrin α3β1 and/or the integrin α6β4 receptor and has been reported to increase resistance to gefitinib, an inhibitor of epidermal growth factor receptor, in HCC cell lines *in vitro* [10]. Whether Ln-332 is part of the CSC niche in hepatic cancer and whether it can influence the behaviour of CSCs remains unclear. In small cell lung cancer Ln-integrin interactions attenuate cell survival and chemoresistance through activation of the mammalian target of rapamycin (mTOR) axis [11]. mTOR has been described as a central regulator of cell growth, metabolism and survival [12]. We therefore hypothesised that mTOR could be potentially involved in regulating the hepatic CSC phenotype.

In this study, we aim to characterise the CSC niche in different histopathological subtypes of hepatic carcinomas, reflecting their possible cell of origin. To isolate putative CSCs, the side population (SP) technique was used (based on the functional ability of the ATP-binding cassette transporters to efflux the fluorescent dye Hoeschst33342), which has proven to be useful in HCC cell lines to isolate cells with a 'stemness' signature that show an increased ability for tumour-initiation and chemoresistance [13–16]. Identification and characterisation of the SP was performed using qPCR and immunohistochemistry. In addition, the influence of Ln-332 on 'stemness' traits, such as chemoresistance and quiescence, and potential downstream targets, such as HPC markers, was investigated *in vitro* and *in vivo*.

Material and methods

Human tissue samples

Eighteen patients diagnosed with an hepatic carcinoma between 2008 and 2012 at the University Hospitals in Leuven (Belgium) were included in this study. Immediately after surgical removal of the tumour (resection samples), part of the tissue was fixed in 6% formalin and embedded in paraffin, while the other part was stored in Recovery™ Cell Culture Freezing Medium (Invitrogen, Carlsbad, CA, USA) in liquid nitrogen. The histopathological diagnosis of HCCs or combined HCC/CCs was performed according to the World Health Organization criteria. Fibrolamellar HCCs were not included. HCCs were further subdivided into K19-negative and K19-positive HCCs as previously described [17]. The study was approved by the ethical committee of the University Hospitals Leuven, Belgium.

Side population analysis

SP analysis was performed as previously published [7]. A detailed description can be found in the Supplementary material. In short, frozen samples were thawed and dissociated using LiberaseBlendzyme 3 (0.8 Wunsch unit/ml, 1.5 h, 37 °C) (Roche, Basel, Switzerland). Single cell suspension was incubated with 5 μg/ml Hoechst33342 (Sigma-Aldrich, St Louis MO, USA) for 90 min at 37 °C. The ABC-transporter inhibitor Verapamil (100 μM; Sigma-Aldrich) was used to assess the SP phenotype from the rest of the main population (MP); propidium iodide (2 μg/ml; Sigma-Aldrich) to exclude dead cells. Samples were analysed using a FACSAriaII (BD Biosciences) under UV excitation (450/50, 675/20 filter).

The size of the SP was calculated as percentage of the total viable population. Median cell size of SP and MP was analysed based on the Forward Scatter Area (FSC-A). Sorted cells were fixed using BD CytoRich™ System (BD Biosciences) and processed into cytospins for Papanicolaou stainings or immunocytochemistry. Part of the sorted cells out of twelve patient samples (four per histological group) was processed for qPCR analysis. The description of the qPCR method and the list of primers can be found in Supplementary material and Supplementary Table 1.

Immunohistochemistry/immunocytochemistry

Five-micrometre-thick human formalin-fixed paraffin-embedded (FFPE) tissue slides and cytospins were stained with the Leica BOND-MAX™ system (Leica Microsystems GmbH, Wetzlar, Germany), using the Novocastra Bond Polymer Detection Kit (Leica). Visualisation was done using DAB-Chromogen, followed by a haematoxylin counterstaining. Cultured primary cells and cell lines were stained using BrightVision Poly-HRP (Immunologic, Duiven, The Netherlands) and visualised with 3-amino-9-ethylcarbazole. Primary antibodies were directed against ABCB1/MDR1 (1/10 for FFPE slides, 1/100 for cytospins; Monosan, Uden, The Netherlands), ABCG2/BCRP (1/5 for FFPE slides, 1/100 for cytospins; Santa Cruz Biotechnology, Dallas, Texas, USA), K19 (1/25; Dako, Glostrup, Denmark), γ2-chain of Ln-332 (1/500; Sigma-Aldrich), Ln-332 (an antibody recognizing the complete protein, 1/100; Abcam, Cambridge, UK), phospho-mTOR (pmTOR, Ser2481; 1/50; Cell Signaling, Danvers, MA, USA) and phospho-Histone H3 (pHH3; 1/100; Millipore, Billerica, MA, USA).

Immunofluorescence

Human FFPE samples were deparaffinised, processed for epitope retrieval and stained for γ2-chain of Ln-332+K19 or γ2-chain of Ln-332+Ki67 (ready-to-use, Dako) for 45 min. Cell culture samples were fixed in 4% formaldehyde solution and stained for K19+pHH3 for 45 min. Afterwards samples were incubated for 30 min with Alexa Fluor® 568 Goat Anti-Rabbit and Alexa Fluor® 488 Goat Anti-Mouse (1/100, Invitrogen). Samples were counterstained with DAPI (Invitrogen). Fluorescent signals were observed using Zeiss Axioplan (Carl Zeiss, Oberkochen, Germany).

In vitro growth potential of primary samples

To assess the *in vitro* growth potential of primary human hepatic cancer, dissociated primary tissue samples (n = 2 per histological group) were grown in Advanced Dulbecco's Modified Eagle's Medium (Invitrogen), supplemented with 10% heat-inactivated Fetal Bovine Serum and L-Glutamine (Invitrogen); at 37 °C in a humidified chamber supplemented with 5% CO_2. Cells that showed growth potential were passed on and characterised by immunocytochemistry at twelve weeks.

In vitro Ln-332 coating experiments

Characterisation cell lines

Human HCC cell lines PLC/PRF/5, HepG2 (ECACC, Salisbury, UK) and Hep3B2 (ATCC-LGC Standards, Molsheim Cedex, France) were grown in similar conditions as the dissociated human samples. Cells were processed into FFPE tissue blocks using the Cellient Automated Cell Block System (Hologic, Bedford, MA, USA) and stained for K19, γ2-chain of Ln-332 and integrin α6 receptor chain (ITGA6; 1/50; Sigma-Aldrich) expression using immunohistochemistry as described above.

mRNA expression

Six-well cell culture plates were coated with Ln-332 (Biolamina, Stockholm, Sweden) at a concentration of 2 μg/cm^2 (1.5 h, 37 °C) and seeded with 6×10^5 HCC cells (n = 3 per cell line). After 72 h the cells were harvested for mRNA extraction and processed for qPCR analysis (Supplementary material).

Protein expression

The effect of Ln-332 on protein expression was accessed using HepG2 cells (n = 4), grown in 8-well cell culture slides, by means of immunocytochemistry (see above). Immunopositive cells were counted in five representative high power fields. Additionally HepG2 cells were treated with mTOR inhibitors rapamycin (10 nM) or WYE-687 (5 μM) (Selleckchem, Tx, USA) and analysed by immunofluorescence. Determination of the IC50 value for WYE-687 in HepG2 cells can be found in Supplementary material and Supplementary Fig.1.

Chemosensitivity

HepG2 cells, grown in coated and non-coated conditions for 72 h, were treated with Doxorubin (1 μM and 20 μM) or Sorafenib (1 μM, 10 μM and 20 μM) (Selleckchem) for 48 h. Proliferative activity was assessed by bromodeoxyuridine (BrdU) labelling (Roche, Mannheim, Germany), according to manufacturer's instructions. Experiments were performed in quadruplicate.

Stemness features

Coated and non-coated HepG2 cells were submitted to SP analysis (n = 3) using 5 μg/ml Hoechst33342 with or without Verapamil at 50 μM (Sigma-Aldrich). Colony forming assays were performed by seeding 500 HepG2 cells in coated and non-coated 6-well plates (n = 3). After ten days, cells were visualised with a Giemsa stain (Sigma-Aldrich) and counted using a brightfield microscope.

Xenograft models

Six- to eight-week-old NOD.CB17-*Prkdc*^{scid}/NCrHsd mice (Harlan, Boxmeer, The Netherlands) were injected subcutaneously with 3×10^6 HepG2 cells in a total volume of 200 μl, consisting of Dulbecco's Modified Eagle's Medium with or without supplement: either Ln-332 (40 μl of the total volume; Biolamina) or Matrigel (100 μl of the total volume; Corning, NY, USA) or both. This categorised the animals into four groups (2 animals per group, injected at both flanks): HepG2, HepG2+Ln-332, HepG2+matrigel and HepG2+matrigel+Ln-332. Upon macroscopic observation of the first tumour nodule, tumour dimensions were measured daily using the following formula: volume (mm^3) = $ab^2/2$, where b was the smaller dimension. All animals were sacrificed at day 10, calculated from the time point when the first tumour nodule was observed. Samples were processed into FFPE blocks and processed for K19-immunostaining and haematoxylin-eosin staining.

Statistical analysis

Statistical qPCR analysis was performed using the Mann-Whitney *U* test, the unpaired/paired Student's *t* test and the two-way mixed ANOVA with GraphPad Prism 5.02 (GraphPad Software, Inc., La Jolla, CA, USA). All analyses were two-tailed. In all cases, $p < 0.05$ was considered significant.

Results

Side population proportion correlates with the degree of hepatic progenitor cell features

Candidate CSCs were isolated using the SP method, a technique based on the functional ability of the ATP-binding cassette transporters to efflux the fluorescent dye Hoeschst33342. Using the ABCB1/MDR1 blocker verapamil, an SP was identified ranging from 0.60 to 32.50%. The hepatic carcinomas were subdivided into three groups corresponding to their presumed cell of origin. Flow cytometric analysis showed that the average SP proportion varied from 3.43% (±2.27) in K19-negative HCCs (n = 7) to 9.29% (±4.42) in K19-positive HCCs (n = 7) and 15.43% (±13.98) in the combined HCC/CC (n = 4); showing that the size of the CSC population inclines with the degree of HPC features (Fig. 1). The SP proportion of K19-negative HCCs was significantly smaller than that of the K19-positive HCCs ($p < 0.01$) and the combined HCC/CC ($p < 0.05$).

To assess the overlap with ABCG2, a transporter which can also be targeted to obtain the SP phenotype, cytospins of sorted human cells were stained for MDR1 and ABCG2 [18]. The SP showed an increased expression of both MDR1 and ABCG2 compared to the MP (Fig. 1). In human FFPE samples, MDR1 as well as ABCG2 showed a gradient of immunoreactivity throughout all the tumour samples, with the strongest in small to intermediate-sized tumour cells (Supplementary Fig. 2). In the non-neoplastic surrounding tissue, MDR1 and ABCG2 were highly expressed in the HPCs.

Analysis of the median cell size of each sample showed that SP contained smaller cells compared to the MP (significantly different in the K19-positive HCC and combined HCC/CC group) (Fig. 1). Morphologically the SP fraction contained small sized cells with a high nucleus-cytoplasm ratio, while the MP contained larger tumour cells with a low nucleus-cytoplasm ratio (Fig. 1).

Side population displays elevated expression of hepatic progenitor cell markers

Sorted samples were analysed by qPCR to examine the purity and to investigate biliary/HPC/stemness features. Compared to the MP, the SP of each group showed significantly elevated expression for the biliary/HPC markers *KRT19*, *KRT7* and *TACSTD2*, the extracellular matrix marker *LAMC2* and the ABC-transporter *MDR1* (Table 1). In addition, the SP of the K19-negative HCCs showed a significantly higher expression compared to their respective MP for *CD133*, *TWEAKR*, *JAG1*, *LAMB1*, *ITGA3*, *ITGB4*, *MUC1* and *ALB*; the SP of the K19-positive HCCs for *EPCAM*, *TWEAKR*, *CXCR4*, *ITGA6* and *ITGB1*; and the SP of the combined HCC/CC for *EPCAM* and *ITGA3*. *ITGA3* was significantly reduced in the SP of K19-positive HCCs. No significant differences were found for the biliary/HPC marker *SOX9* or the ABC-transporters *MRP1*, *MRP2*, *MRP3* and *ABCF2*. The mesenchymal markers *VIM* and *aSMA*, the hematopoietic marker *CD45* and the endothelial marker *CD31* were not significantly differentially expressed, suggesting that these cell types are not overrepresented in either SP or MP. A comparison of the different SP fractions for each group can be found in Supplementary Fig. 3.

γ2-chain of Ln-332 immunopositivity correlates with K19 expression and a low proliferation ratio

Since mRNA expression levels of the biliary/HPC marker *KRT19* and the extracellular matrix marker *LAMC2* (encoding the γ2-chain of Ln-332) were upregulated in the SP of each histological group, we aimed to analyse their protein expression *in vivo* using immunohistochemistry. As expected, K19-negative HCCs showed no positivity for K19 on protein levels (Fig. 2), while immunoreactivity for the γ2-chain of Ln-332 was only observed focally in the cytoplasm and in the surrounding of small tumour cells. In K19-positive HCCs, K19 displayed a submembranous staining pattern, prominently in small to intermediate-sized cells (Fig. 2). The γ2-chain staining pattern was similar to K19-negative HCCs, though the number of positive cells was noticeably higher in the K19-positive HCCs. Combined HCC/CCs showed a strong immunopositivity for K19 in the cholangiocytic differentiated area and the ductular area, and a scattered positivity in the hepatocytic differentiated area (Fig. 2). The γ2-chain of Ln-332 was prominently expressed in the ductular area. In the surrounding non-tumoural tissue, the γ2-chain was seen as part of the extracellular matrix surrounding the K19-positive HPCs. Focally,

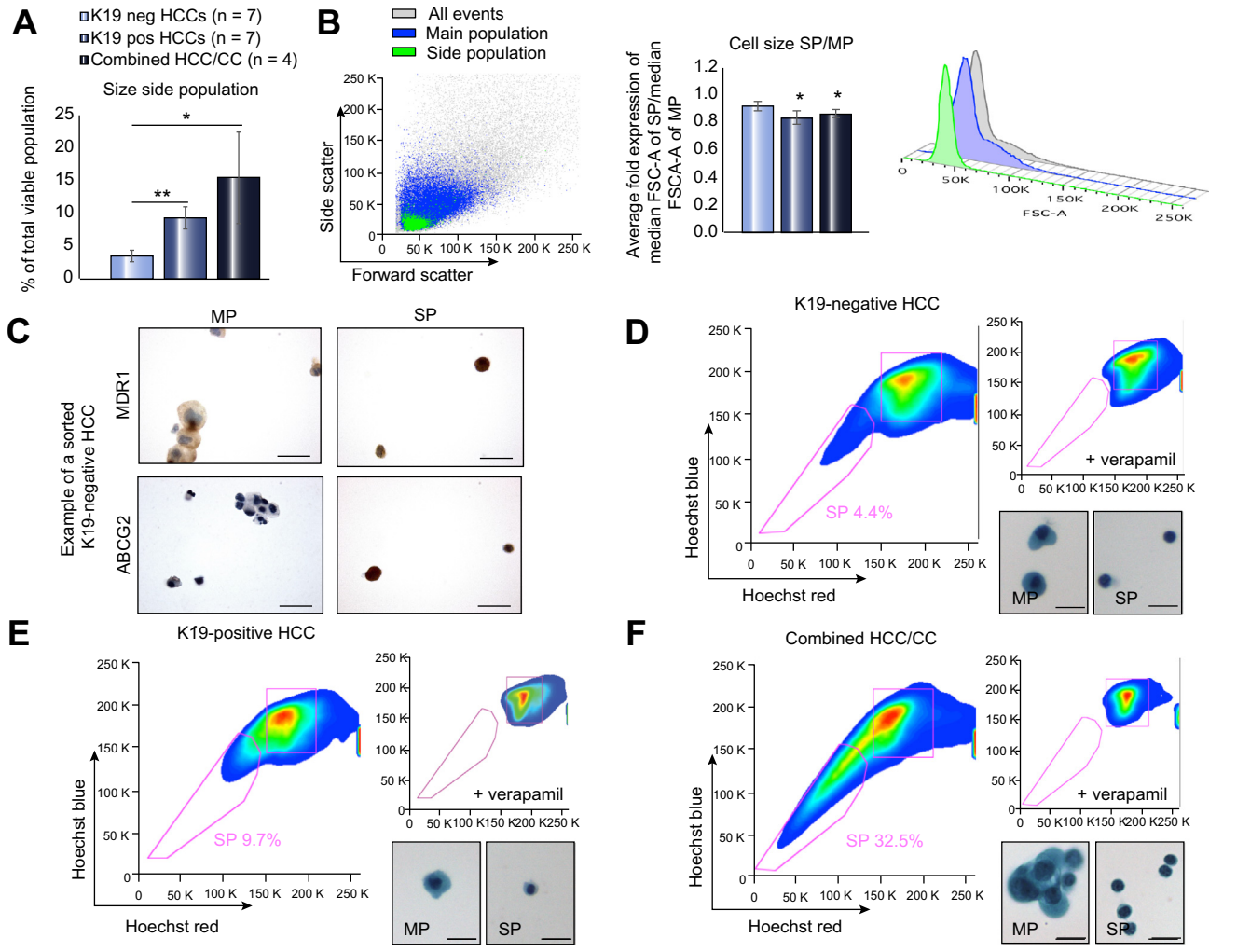


Fig. 1. Side population (SP) in human hepatic carcinomas. SP phenotype is based on the functional ability of stem-like cells to efflux the fluorescent dye Hoechst3342. The ABC-transporter blocker verapamil was used as a control. (A) Flow cytometric analysis showed that the mean SP proportion in the hepatic carcinomas gradually increased with the degree of HPC features (unpaired Student's *t* test; $^{**}p$ <0.01; $^{*}p$ <0.05). (B) Median cell size was calculated for each sample based on the Forward Scatter Area (FSC-A). Results are displayed as average fold FSC-A of the SP compared to the main population (MP) for each histological group (paired Student's *t* test; $^{*}p$ <0.05). Flow cytometry plots show the SP, MP and all events of a representative K19-positive HCC. (C) Immunocytochemistry for MDR1 and ABCG2 was performed on the sorted SP and MP of each human sample (n = 18). Panel (C) shows the MRD1 and ABCG2 expression in a representative sorted K19-negative HCC sample. (D–F) Representative example of a SP plot of the different histological subtypes. Morphologically the SP fraction contained small to intermediate-sized cells with scan cytoplasm, while the MP contained larger tumour cells (Scale bars 50 μm).

a single HPC was observed to show cytoplasmic positivity for the γ2-chain of Ln-332 (Fig. 2, arrow). Additionally, γ2-chain immunopositivity was noted in parts of the inflammatory cells and endothelial cells in both tumour tissue as surrounding liver tissue.

Immunofluorescent double stainings showed that K19 and the γ2-chain of Ln-332 were strongly co-expressed in the ductular area of the combined HCC/CCs, whereas the γ2-chain was low in the hepatocytic differentiated area where a gradual loss of K19 was noted (Fig. 3A). Moreover, in areas where the γ2-chain of Ln-332 was strongly present, the Ki67 nuclear positivity was reduced, indicating a lower proliferation rate (Fig. 3A).

Only the dissociated primary combined HCC/CCs showed capacity to survive in standard cell culture conditions. Characterisation by immunocytochemistry (at passage 12) revealed that these cells were positive for K19, the γ2-chain of Ln-332 and the complete protein Ln-332 (Fig. 3B).

Ln-332 induces K19 expression, quiescence and chemoresistance in vitro

In view of the strong correlation between the γ2-chain of Ln-332 and HPC morphology (K19 expression and low proliferation index), we focused on the influence of Ln-332 *in vitro* to assess whether it has a direct effect on 'stemness' features of hepatic carcinomas. The Hep3B2 cell line was found to be positive for K19, γ2-chain of Ln-332 and integrin α6 (ITGA6) (Fig. 4A). HepG2 showed focal positivity for K19, low to no expression for the γ2-chain and strong positivity for ITGA6. PLC/PRF/5 was negative for all three markers. After a period of 72 h, Ln-332 coating

Table 1. Side population displays elevated expression of hepatic progenitor cell markers.

Gene	Description	Fold expression SP/MP		
		K19 neg HCCs	K19 pos HCCs	Combined HCC/CC
Progenitor cell markers				
KRT19	Keratin 19	2.90 (p <0.05)	4.82 (p <0.05)	6.28 (p <0.01)
KRT7	Keratin 7	7.14 (p <0.05)	8.99 (p <0.05)	5.47 (p <0.05)
EPCAM	Epithelial cell adhesion molecule	1.52	4.67 (p <0.05)	2.02 (p <0.01)
TACSTD2/TROP2	Tumor-associated calcium signal transducer 2	22.32 (p <0.01)	5.52 (p <0.05)	7.50 (p <0.05)
PROM1/CD133	Prominin 1	7.50 (p <0.05)	201.2	1.22
SOX9	SOX9 SRY (sex determining region Y)-box 9	3.24	0.82	1.36
TNFRSF12A/TWEAKR	Tumor necrosis factor receptor superfamily, member 12A	5.60 (p <0.01)	2.31 (p <0.05)	2.3
CXCR4	Chemokine (C-X-C motif) receptor 4	0.71	3.19 (p <0.05)	0.84
JAG1	Jagged 1 (Alagille syndrome)	10.67 (p <0.05)	1.65	2.98
ATP-binding cassette transporters				
ABCB1/MDR1	ATP-binding cassette, sub-family B (MDR/TAP), member 1	1.81 (p <0.05)	10.11 (p <0.05)	6.45 (p <0.05)
ABCC1/MRP1	ATP-binding cassette, sub-family C (CFTR/MRP), member 1	1.36	6.24	0.47
ABCC2/MRP2	ATP-binding cassette, sub-family C (CFTR/MRP), member 2	42.29	20.3	0.27
ABCC3/MRP3	ATP-binding cassette, sub-family C (CFTR/MRP), member 3	19.61	35.68	2.41
ABCF2	ATP-binding cassette, sub-family F (GCN20), member 2	2.68	1.71	0.12
Laminin and integrin receptors				
LAMB1	Laminin, beta 1	4.40 (p <0.05)	8.14	0.31
LAMC2	Laminin, gamma 2	18.54 (p <0.01)	6.12 (p <0.05)	15.63 (p <0.05)
ITGA3	Integrin, alpha 3	11.85 (p <0.01)	0.04 (p <0.05)	2.10 (p <0.05)
ITGA6	Integrin, alpha 6	1.53	10.49 (p <0.01)	1.7
ITGB1	Integrin, beta 1	1.23	3.87 (p <0.05)	0.58
ITGB4	Integrin, beta 4	2.95 (p <0.01)	2.26	1.04
Biliary marker				
MUC1/EMA	Mucin 1, cell surface associated	9.98 (p <0.05)	2.72	4.05
Hepatocytic marker				
ALB	Albumin	6.13 (p <0.05)	1.36	1.78
Mesenchymal markers				
VIM	Vimentin	0.75	1.21	1.23
Endothelial marker				
PECAM1/CD31	Platelet/endothelial cell adhesion molecule	0.37	0.41	0.37
Hematopoietic marker				
PTPRC/CD45	Protein tyrosine phosphatase, receptor type, C	0.38	2.63	0.21

significantly increased mRNA expression of *KRT19*, *TACSTD2* and *KLF4* in HepG2, and *KRT19*, *EPCAM*, *CD133/PROM1* and *JAG1* expression in Hep3B2 cells. No differences were noticed in the PLC/PRF/5 cell line (Fig. 4B).

Using HepG2 as a model focally positive for K19 and low/negative for the γ2-chain of Ln-332, Ln-332 coating increased the number of K19-positive tumour cells and the phosphorylation of mTOR (Ser2481), and reduced the expression of the mitotic marker pHH3 (Fig. 4C, D). Morphologically, coated cells grew less in clusters and had irregular shapes with extended filopodia formation. Treatment (72 h) of coated HepG2 cells with rapamycin (mTORC1 inhibitor) ameliorated the effect of Ln-332, more K19 and less pHH3 expression, while treatment with WYE-687 (mTORC1+C2 inhibitor) diminished this effect (Fig. 4D, E).

After 72 h Ln-332 coated HepG2 cells displayed an increased SP fraction of 3.00 ± 1.28% compared to 0.17 ± 0.15% found in non-coated cells (Fig. 4F). Additionally Ln-332 coating significantly increased resistance to doxorubicin (20 μM) or sorafenib (10 μM and 20 μM) treatment (Fig. 4G).

HepG2 cell colony formation assays showed that Ln-332 improved survivability after a period of ten days. Intriguingly, the growth pattern of the coated cells was observed as scattered single cells rather than clonogenic colonies, suggesting induction of cell quiescence (Fig. 5A).

Ln-332 delays tumour growth and sustains K19 expression in vivo

The *in vivo* effect of Ln-332 was investigated in a subcutaneous xenograft model injected using HepG2 cells with or without matrigel and/or Ln-332. Tumour formation was observed in both flanks of each animal, with the exception of one animal (HepG2 +Ln-332 group), which only formed a tumour on one flank.

Four weeks after tumour inoculation, tumour growth was first observed in an animal injected with HepG2+matrigel. From that time point all animals were monitored daily for a total period of ten days and then sacrificed. Ln-332 significantly reduced tumour growth either with or without matrigel injection (Fig. 5B, C). Mixed model ANOVA analysis of the growth curves can be found in Supplementary Table 2. Morphologically, tumours injected with Ln-332 displayed more stromal and microvascular invasion, as well as invasion in the underlying muscular layer, compared to the tumours that were not injected

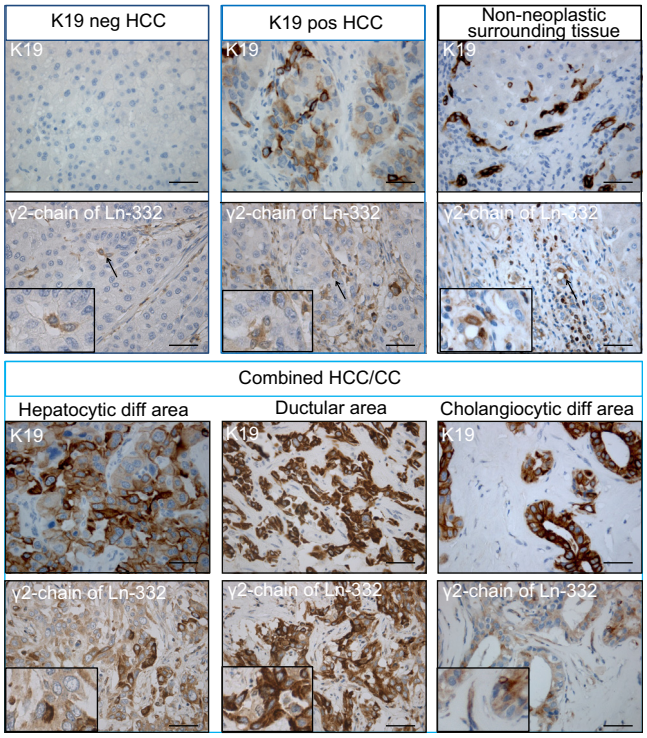


Fig. 2. Immunohistochemical staining for K19 and the γ2 chain of Ln-332 in human hepatic carcinomas. Upper panel displays a representative example of a K19-negative HCC (total stained samples n = 7), a K19-positive HCC (n = 7) and non-neoplastic surrounding liver tissue (n = 18). Arrows indicate cells positive for γ2 chain of Ln-332. Lower panel displays a representative example of a combined HCC/CC (n = 4), subdivided in areas of hepatocytic differentiation (diff), cholangiocytic diff or ductular areas (Scale bars 100 μm).

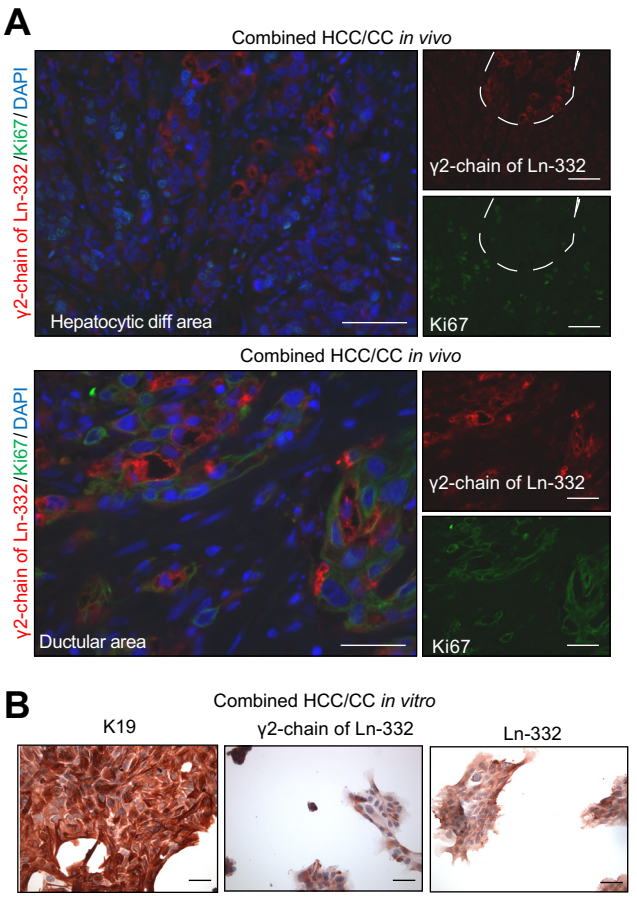


Fig. 3. Expression of γ2-chain of Ln-332 correlates with K19 and a low proliferation rate. (A) Immunofluorescent double staining for the γ2-chain of Ln-332 and K19, or the γ2- chain of Ln-332 and Ki67 in a combined HCC/CC. (n = 4, Scale bar 100 μm). (B) Only the combined HCC/CCs showed capacity to grow *in vitro* (n = 2). Immunohistochemical analysis was performed in triplicate on passage 12 for K19, the γ2-chain of Ln-332 and the complete Ln-332 (Scale bar 200 μm).

with Ln-332 (Fig. 5C; Supplementary Fig.4). In addition, tumours injected with Ln-332 showed a higher expression of K19, which appears scattered throughout the tumour with a concentration at the invasive front (Fig. 5D; Supplementary Fig.4).

Discussion

Current therapeutic strategies for the treatment of hepatic cancer mostly focus on the inhibition of tumour growth, though the results are often unsatisfactory [19]. A prerequisite for the development of new therapies is a good understanding of tumour behaviour and, in particular, understanding the resistant CSC population. The occurrence of HPC markers in hepatic cancer (e.g. HCCs) has been used for prognostic stratification, however to date the relationship between CSCs and HPC features remains unclear [20]. In this study we showed that the size of the CSC fraction (isolated based on the functionality of their ABC-transporters) gradually increases with the degree of HPC features found in hepatic carcinomas, reflecting the possible cell of origin. Holczbauer *et al.* recently found similar results in mice, reporting that the SP/CSC population is the largest in cell lines derived from HPCs, when comparing immortalized cell lines from different hepatic lineage (e.g. hepatocytes, HPCs and hepatoblasts) [21]. One important player that determines the behaviour of stem cells in general is their specialised microenvironment [22]. We especially focused our study on the role of the γ2-chain of Ln-332 as our group previously showed that its expression was associated with HPC features in HCCs and as other groups described it as a poor prognosis indicator in hepatic cancer [7,23]. Importantly, this current study showed that the γ2-chain was part of the neoplastic CSC niche, as well as the non-neoplastic HPC niche, more specifically in tumour areas with a low proliferation rate and high K19 expression. *In vitro*, Ln-332 induced a phenotype switch in hepatic carcinoma cells by pushing them towards a more quiescent cell state and a more biliary/HPC phenotype [24,25]. The Ln-332-induced cell phenotype interestingly proved to be more resistant to doxorubicin and sorafenib treatment. Quiescence and chemoresistance are regarded as typical characteristics of both CSCs as well as normal stem cells [26]. Previous studies in glioblastoma, colorectal and pancreatic cancer showed that slow-cycling tumour cells in a reversible state of quiescence are actually responsible for chemoresistance and recurrence [27–29]. Remarkably, Ln-332 not only protects hepatic cancer cells against chemotherapy but stimulates cell proliferation upon sorafenib exposure. In xenograft mouse models

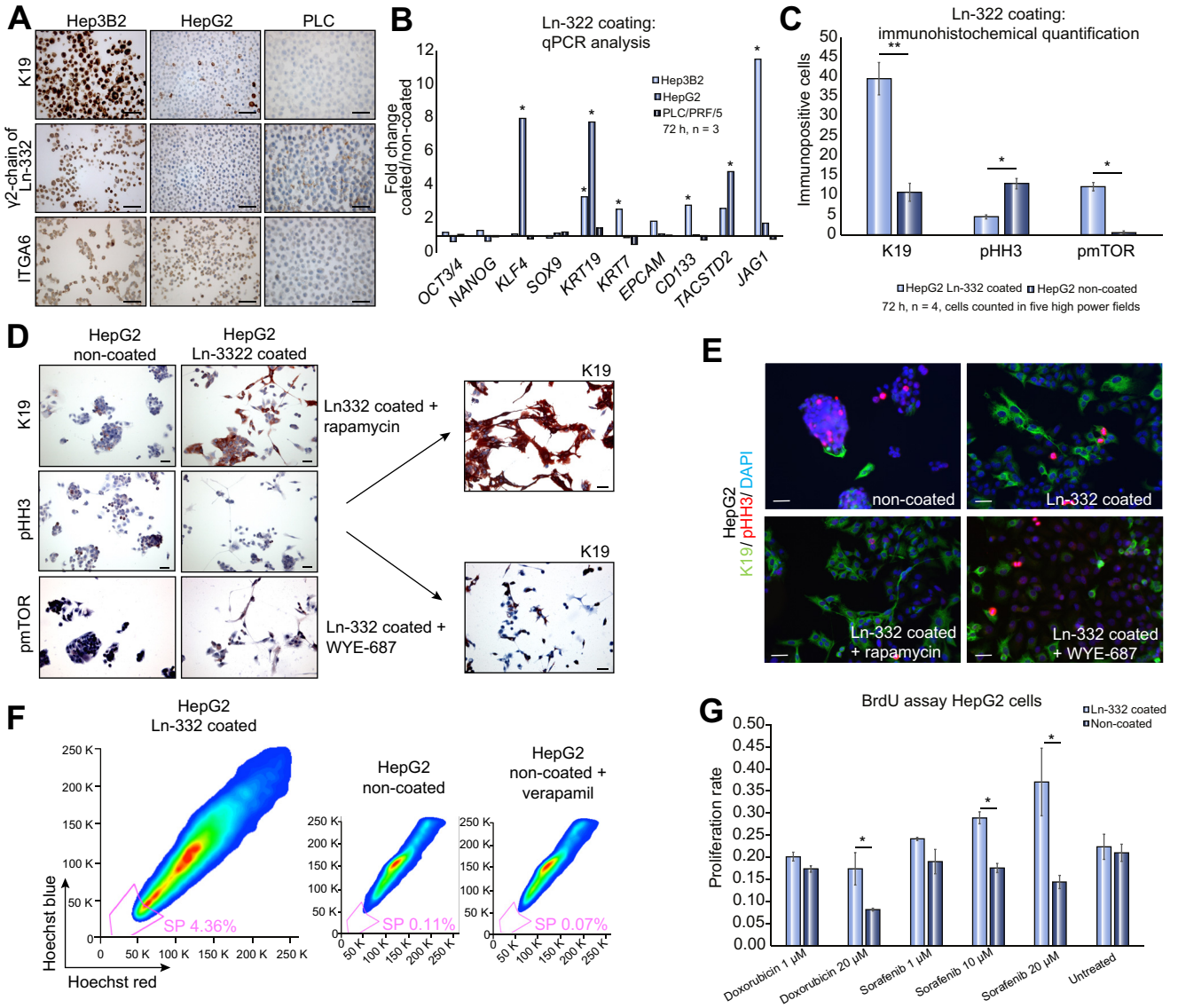
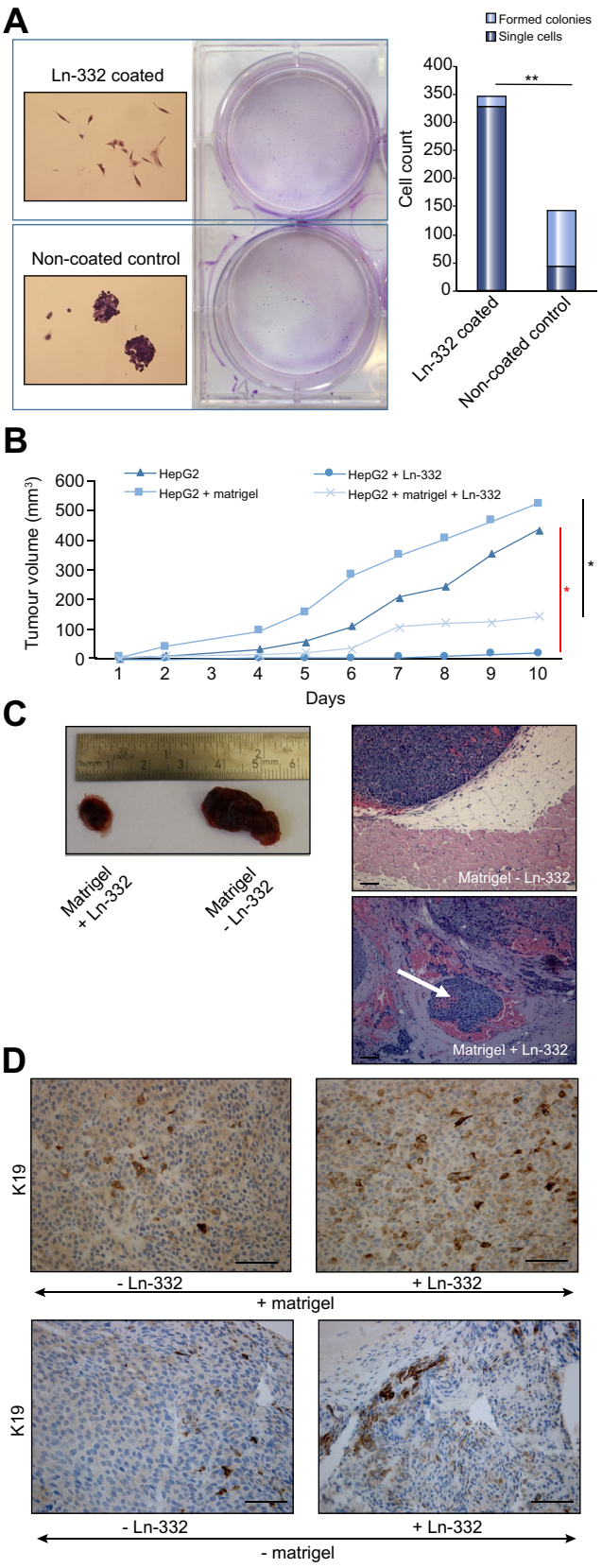


Fig. 4. Ln-332 induces K19 expression, quiescence and chemoresistance *in vitro*. (A) Hep3B2, HepG2 and PLC/PRF/5 HCC cell lines were characterised for K19, the γ2-chain of Ln-332 and integrin α6 (ITGA6) expression. (B) The effect of Ln-332 (t = 72 h) coating on mRNA expression of the Hep3B2, HepG2 and PLC/PRF/5 cells was analysed using qPCR. Results are displayed as relative fold expression, normalised to housekeeping genes (n = 3 per cell line) (Mann-Whitney *U* test; $^{*}p$ <0.05). (C, D) The effect of Ln-332 coating on K19, phospho-histone H3 (pHH3) protein and phosphorylated mTOR (pmTOR Ser2481) expression in HepG2 cells (n = 4) was visualised with immunocytochemistry. Immunopositive cells were counted in five high power fields (Mann-Whitney *U* test; $^{**}p$ <0.01; $^{*}p$ <0.05). (D) mTOR inhibitors rapamycin and WYE-687 were added to the cell culture medium of Ln-332 coated HepG2 cells (72 h, n = 4). The effect on K19 was analysed by immunocytochemistry. (E) Immunofluorescent double staining for K19 and pHH3 on HepG2 cells in non-coated condition, Ln-332 coated condition or Ln-332 coated condition supplemented with mTOR inhibitors (either rapamycin or WYE-687; n = 4). (F) The effect of Ln-332 coating on the SP phenotype in HepG2 cells was analysed using the fluorescent dye Hoechst3342 and the ABC-transporter blocker verapamil (n = 3). (G) Coated and non-coated HepG2 cells (t = 72 h) were submitted to a doxorubicin (1 μM and 20 μM) and sorafenib (1 μM, 10 μM and 20 μM) treatment for 48 h (n = 4). The proliferation rate was assessed using a BrdU incorporation assay. (Scale bars 100 μm) (Mann-Whitney *U* test; $^{**}p$ <0.01; $^{*}p$ <0.05).

derived from primary urothelial carcinomas, cytotoxic chemotherapy induces proliferation of a sub-fraction of the tumour cells, more preciously the K14-positive ones, despite the reduction seen in the tumour size [30]. So it might be possible that Ln-332 induces quiescence in hepatic cancer under 'normal' circumstances and that once under cellular stress (e.g. sorafenib treatment) these cells react by enhanced proliferating.

Laminin-mediated activation of the mTOR pathway has been reported to induce cell survival and chemoresistance in small cell lung cancer [11]. The mTOR kinase has multiple downstream effects depending on which distinct protein complex it forms, termed mTORC1 and mTORC2 [31]. The mTORC1 complex promotes cell growth by inducing metabolic processes in response to nutrients and oxygen, whereas the mTORC2 complex responds to growth factors and regulates cell survival, as well as the cytoskeleton [12]. Our study shows that the effect of Ln-332 is mTORC2-dependent, which is further enhanced upon mTORC1 inhibition (more K19 expression and quiescence). Presumably,



there is a shift towards mTORC2 activation, driving the cells into 'survival mode'.

Rictor, a binding partner of the mTORC2 complex, has recently been linked with early recurrence after curative treatment and poor overall survival in patients diagnosed with HCC [32]. Marquardt *et al.* reported that when treating HCC cell lines with zebularine, a DNA methyltransferase-1 inhibitor, the SP fractions showed a differential expression of Rictor, associated with an increase in the expression of biliary/HPC cell markers (e.g. *KRT19*) [16]. The possible link between mTORC2 and Ln-332-induced phenotype switching could have a huge impact on current on-going clinical trials. It might explain why rapamycin, a specific mTORC1 inhibitor, fails its benefit as adjuvant therapy, as it presumably misses its effect on CSCs.

Even though we found a CSC fraction in each histological group, Ln-332 failed to induce 'stemness' markers in the PLC/PRF/5 cell line, characterised as K19-negative. The lack of expression of the ITGA6, one of the receptor subunits for Ln-332, in this cell line could explain why no differences were observed. The presence or absence of specific markers/receptors might reflect the cell of origin [33].

The SP of the K19-positive HCCs is unique in its high expression of *CXCR4*, a typical CSC marker linked with lymph node metastasis and poor survival in human HCCs [34]. CXCR4 expression was observed at the tumour border as well as in small cells scattered in the tumour bulk, similar to the K19 expression pattern as seen in the human samples and in the xenograft models (Supplementary material). This underlines the complex nature of CSCs. Further research in localisation of CSCs and how they interact with their environment will be necessary.

The future challenge in treatment of hepatic cancer will not only be to reduce tumour growth, but also to target CSCs and their specialised niche. As the CSC phenotype differs depending on the histological subtype, a more personalised treatment would be required for each individual patient diagnosed with hepatic cancer.

Our study demonstrates that tumour behaviour is plastic and depends on the microenvironment of the tumour cell. We particularly identified an important role for Ln-332 and more specifically its γ2-chain as part of the specialised CSC niche in maintaining and supporting 'stemness', e.g. quiescence and chemoresistance. Therefore, monoclonal antibody treatment targeting the γ2-chain of Ln-332 could provide an innovative therapy of hepatic cancer.

Fig. 5. Ln-332 promotes survival and delays tumour growth. (A) Colony forming assay for HepG2 cells in coated and non-coated condition (t = 10 d, n = 3). Cells were visualised and quantified for each well (unpaired Student's *t* test; $^{**}p$ <0.01). (B) HepG2 cells were subcutaneously injected in NOD/SCID mice. Animals were categorised into four groups: HepG2, HepG2+Ln-332, HepG2 +matrigel and HepG2+matrigel+Ln-332. After four weeks tumour growth was observed. From that time point all animals were monitored daily for a total period of ten days and then sacrificed. (Mixed model ANOVA; $^{*}p$ <0.05; detailed statistical analysis: see Supplementary material). (C) Macroscopic picture (left) and haematoxylin-eosin staining (right) of xenograft tumours obtained from HepG2+matrigel injected either with or without Ln-332. Arrow indicates microvascular invasion. (D) Immunohistochemistry was used to examine the effect of Ln-332 on K19 expression in the xenograft models (Scale bars 200 μm).

Financial support

This study was supported by a grant from the Belgian Federal Science Policy Office (Interuniversity Attraction Poles program – P6/20 and P7/83-HEPRO), the Fund of Scientific Research Flanders FWO G.0348.13N and the Austrian Science Fund (FWF), T597 (MP) and FWF P25356 (WM).

Conflict of interest

The authors who have taken part in this study declared that they do not have anything to disclose regarding funding or conflict of interest with respect to this manuscript.

Authors' contributions

OG and TR designed the study. OG, JW, MP, YV, KVD, AC, GG, HVV, WM collected and analysed *in vitro* and *in vivo* data. OG, SV, LD, LG, LVG, HV performed SP analysis. OG, AVDB, FN, BT, MK, TR included patients. MK and TR performed histological classification. OG and TR drafted the manuscript.

All authors revised the manuscript critically for intellectual content, and have approved the final version.

Acknowledgements

The authors would like to thank Prof. Dr. Valeer J. Desmet, Prof. Dr. Joost van den Oord, Christophe Empsen and Paula Aertsen for their indispensable support.

Supplementary data

Supplementary data associated with this article can be found, in the online version, at http://dx.doi.org/10.1016/j.jhep.2015.11.011.

References

[1] Beck B, Blanpain C. Unravelling cancer stem cell potential. Nat Rev Cancer 2013;13:727–738.
[2] Roskams T. Liver stem cells and their implication in hepatocellular and cholangiocarcinoma. Oncogene 2006;25:3818–3822.
[3] Roskams TA, Libbrecht L, Desmet VJ. Progenitor cells in diseased human liver. Semin Liver Dis 2003;23:385–396.
[4] Kallis YN, Robson AJ, Fallowfield JA, Thomas HC, Alison MR, Wright NA, et al. Remodelling of extracellular matrix is a requirement for the hepatic progenitor cell response. Gut 2011;60:525–533.
[5] Lorenzini S, Bird TG, Boulter L, Bellamy C, Samuel K, Aucott R, et al. Characterisation of a stereotypical cellular and extracellular adult liver progenitor cell niche in rodents and diseased human liver. Gut 2010;59:645–654.
[6] Givant-Horwitz V, Davidson B, Reich R. Laminin-induced signaling in tumor cells. Cancer Lett 2005;223:1–10.
[7] Govaere O, Komuta M, Berkers J, Spee B, Janssen C, de Luca F, et al. Keratin 19: a key role player in the invasion of human hepatocellular carcinomas. Gut 2014;63:674–685.
[8] Sulpice L, Rayar M, Desille M, Turlin B, Fautrel A, Boucher E, et al. Molecular profiling of stroma identifies osteopontin as an independent predictor of poor prognosis in intrahepatic cholangiocarcinoma. Hepatology 2013;58:1992–2000.
[9] Giannelli G, Fransvea E, Bergamini C, Marinosci F, Antonaci S. Laminin-5 chains are expressed differentially in metastatic and nonmetastatic hepatocellular carcinoma. Clin Cancer Res 2003;9:3684–3691.
[10] Giannelli G, Azzariti A, Fransvea E, Porcelli L, Antonaci S, Paradiso A. Laminin-5 offsets the efficacy of gefitinib ('Iressa') in hepatocellular carcinoma cells. Br J Cancer 2004;91:1964–1969.
[11] Tsurutani J, West KA, Sayyah J, Gills JJ, Dennis PA. Inhibition of the phosphatidylinositol 3-kinase/Akt/mammalian target of rapamycin pathway but not the MEK/ERK pathway attenuates laminin-mediated small cell lung cancer cellular survival and resistance to imatinib mesylate or chemotherapy. Cancer Res 2005;65:8423–8432.
[12] Laplante M, Sabatini DM. MTOR signaling in growth control and disease. Cell 2012;149:274–293.
[13] Chiba T, Kita K, Zheng YW, Yokosuka O, Saisho H, Iwama A, et al. Side population purified from hepatocellular carcinoma cells harbors cancer stem cell-like properties. Hepatology 2006;44:240–251.
[14] Chiba T, Miyagi S, Saraya A, Aoki R, Seki A, Morita Y, et al. The polycomb gene product BMI1 contributes to the maintenance of tumor-initiating side population cells in hepatocellular carcinoma. Cancer Res 2008;68:7742–7749.
[15] Hu C, Li H, Li J, Zhu Z, Yin S, Hao X, et al. Analysis of ABCG2 expression and side population identifies intrinsic drug efflux in the HCC cell line MHCC-97L and its modulation by Akt signaling. Carcinogenesis 2008;29:2289–2297.
[16] Marquardt JU, Raggi C, Andersen JB, Seo D, Avital I, Geller D, et al. Human hepatic cancer stem cells are characterized by common stemness traits and diverse oncogenic pathways. Hepatology 2012;54:1031–1042.
[17] Durnez A, Verslype C, Nevens F, Fevery J, Aerts R, Pirenne J, et al. The clinicopathological and prognostic relevance of cytokeratin 7 and 19 expression in hepatocellular carcinoma. A possible progenitor cell origin. Histopathology 2006;49:138–151.
[18] Golebiewska A, Brons NH, Bjerkvig R, Niclou SP. Critical appraisal of the side population assay in stem cell and cancer stem cell research. Cell Stem Cell 2011;8:136–147.
[19] Yamashita T, Wang XW. Cancer stem cells in the development of liver cancer. J Clin Invest 2013;123:1911–1918.
[20] Bruix J, Gores GJ, Mazzaferro V. Hepatocellular carcinoma: clinical frontiers and perspectives. Gut 2014;63:844–855.
[21] Holczbauer A, Factor VM, Andersen JB, Marquardt JU, Kleiner DE, Raggi C, et al. Modeling pathogenesis of primary liver cancer in lineage-specific mouse cell types. Gastroenterology 2013;145:221–231.
[22] Borovski T, De Sousa E, Melo F, Vermeulen L, Medema JP. Cancer stem cell niche: the place to be. Cancer Res 2011;71:634–639.
[23] Giannelli G, Rani B, Dituri F, Cao Y, Palasciano G. Moving towards personalised therapy in patients with hepatocellular carcinoma: the role of the microenvironment. Gut 2014;63:1668–1676.
[24] Pérez-Cadahía B, Drobic B, Davie JR. H3 phosphorylation: dual role in mitosis and interphase. Biochem Cell Biol 2009;87:695–709.
[25] Cheung TH, Rando TA. Molecular regulation of stem cell quiescence. Nat Rev Mol Cell Biol 2013;14:329–340.
[26] Maugeri-Saccà M, Vigneri P, De Maria R. Cancer stem cells and chemosensitivity. Clin Cancer Res 2011;17:4942–4947.
[27] Dembinski JL, Krauss S. Characterization and functional analysis of a slow cycling stem cell-like subpopulation in pancreas adenocarcinoma. Clin Exp Metastasis 2009;26:611–623.
[28] Touil Y, Igoudjil W, Corvaisier M, Dessein AF, Vandomme J, Monté D, et al. Colon cancer cells escape 5FU chemotherapy-induced cell death by entering stemness and quiescence associated with the c-Yes/YAP axis. Clin Cancer Res 2014;20:837–846.
[29] Campos B, Gal Z, Baader A, Schneider T, Sliwinski C, Gassel K, et al. Aberrant self-renewal and quiescence contribute to the aggressiveness of glioblastoma. J Pathol 2014;234:23–33.
[30] Kurtova AV, Xiao J, Mo Q, Pazhanisamy S, Krasnow R, Lerner SP, et al. Blocking PGE2-induced tumour repopulation abrogates bladder cancer chemoresistance. Nature 2014;517:209–213.
[31] Matter MS, Decaens T, Andersen JB, Thorgeirsson SS. Targeting the mTOR pathway in hepatocellular carcinoma: current state and future trends. J Hepatol 2014;60:855–865.
[32] Kaibori M, Shikata N, Sakaguchi T, Ishizaki M, Matsui K, Iida H, et al. Influence of rictor and raptor expression of mTOR signaling on long-term outcomes of patients with hepatocellular carcinoma. Dig Dis Sci 2014;60:919–928.
[33] Govaere O, Roskams T. Pathogenesis and prognosis of hepatocellular carcinoma at the cellular and molecular levels. Clin Liver Dis 2015;19:261–276.
[34] Xiang ZL, Zeng ZC, Tang ZY, Fan J, Zhuang PY, Liang Y, et al. Chemokine receptor CXCR4 expression in hepatocellular carcinoma patients increases the risk of bone metastases and poor survival. BMC Cancer 2009;9:176.